

Associated functional network development and language abilities in children

Ting Qi^{a,*}, Gesa Schaadt^{a,b}, Angela D. Friederici^a

^a Department of Neuropsychology, Max Planck Institute for Human Cognitive and Brain Sciences, Leipzig, Germany

^b Department of Education and Psychology, Free University of Berlin, Berlin, Germany

ARTICLE INFO

Keywords:

Language development
Sentence comprehension
Brain development
Resting-state functional connectivity
Young children
Prefrontal cortex

ABSTRACT

During childhood, the brain is gradually converging to the efficient functional architecture observed in adults. How the brain's functional architecture evolves with age, particularly in young children, is however, not well understood. We examined the functional connectivity of the core language regions, in association with cortical growth and language abilities, in 175 young children in the age range of 4 to 9 years. We analyzed the brain's developmental changes using resting-state functional and T1-weighted structural magnetic resonance imaging data. The results showed increased functional connectivity strength with age between the pars triangularis of the left inferior frontal gyrus and left temporoparietal regions (Cohen's $d = 0.54$, $CI: 0.24 - 0.84$), associated with children's language abilities. Stronger functional connectivity between bilateral prefrontal and temporoparietal regions was associated with better language abilities regardless of age. In addition, the stronger functional connectivity between the left inferior frontal and temporoparietal regions was associated with larger surface area and thinner cortical thickness in these regions, which in turn was associated with superior language abilities. Thus, using functional and structural brain indices, coupled with behavioral measures, we elucidate the association of functional language network development, language ability, and cortical growth, thereby adding to our understanding of the neural basis of language acquisition in young children.

1. Introduction

A core language comprehension network, mainly involving left inferior frontal and left superior temporal regions, has been consistently reported in previous studies with adults (Ferstl et al., 2008; Friederici, 2011; Vigneau et al., 2006). Such perisylvian activation has also been shown in young infants and toddlers listening to auditorily presented sentences (Dehaene-Lambertz et al., 2006; Redcay et al., 2008). Further, regarding children's language development, a body of neuroimaging studies has shown bilateral activation in temporal regions, as well as the pars triangularis of the inferior frontal gyrus (IFG). Despite these brain regions also showing activation in the adult brain, the activation pattern in children differs. For instance, compared to the bilateral activation in children, adult activation has mainly been found in the left pars opercularis of the IFG and in the left temporal gyrus (Enge et al., 2020).

The critical role of age in the development of language comprehension, and related brain regions, is supported by findings that show an age-dependent increase in brain activation in largely distributed bilateral superior and middle temporal regions, which are parts

of the receptive sentence-comprehension network (Weiss-Croft and Baldeweg, 2015). More specifically, converging functional magnetic resonance imaging (fMRI) studies on children's language development have revealed activation of the left superior temporal gyrus (STG) to be present very early in infants (Dehaene-Lambertz et al., 2006; Redcay et al., 2008). Brain activation of the left STG during language comprehension tasks and resting state was also found to be associated with age in children between the ages of 3 and 18 years (Schmithorst et al., 2006; Szaflarski et al., 2012; Wu et al., 2016; Xiao et al., 2016a). These studies indicate the left superior temporal cortex, known to be involved in integrating semantic and syntactic information into an overall sentence meaning, also plays an important role in early language acquisition (for a review, see Friederici, 2011). Moreover, activation of the left STG extends to inferior parietal cortex and is assumed to be, particularly in children, a working memory storage substrate for phonology and syntax (Brauer and Friederici, 2007; Fengler et al., 2016; Friederici, 2011; Knoll et al., 2012; Leff et al., 2009; Meyer et al., 2012; Novais-Santos et al., 2007). The functional language network then gradually extends to more anterior regions during development, such as the left IFG (Friederici et al., 2011; Newman et al.,

* Corresponding author at: Department of Neuropsychology, Max Planck Institute for Human Cognitive and Brain Sciences, Stephanstrasse 1a, Leipzig, 04103, Germany.

E-mail addresses: tingqi@cbs.mpg.de, Ting.Qi@ucsf.edu (T. Qi).

<https://doi.org/10.1016/j.neuroimage.2021.118452>.

Received 9 March 2021; Received in revised form 14 July 2021; Accepted 3 August 2021

Available online 4 August 2021.

1053-8119/© 2021 The Authors. Published by Elsevier Inc. This is an open access article under the CC BY-NC-ND license (<http://creativecommons.org/licenses/by-nc-nd/4.0/>)

2003; Skeide et al., 2014). Specifically, in contrast to the left STG, the left IFG is not yet involved in sentence comprehension in young children (Wang et al., 2019; Wu et al., 2016). In particular, the pars opercularis of the left IFG (i.e., the core region for sentence processing in adults) has not been observed to be involved in sentence processing until early adolescence. Rather, children seem to rely more on the left pars triangularis (Brauer et al., 2011; Skeide et al., 2014; Yeatman et al., 2010). Additionally, functional connectivity studies have also revealed age-related changes of the connection between the left IFG, inferior parietal cortex, and the temporal gyrus during narrative comprehension with increasing connectivity in children between the ages of 5 and 18 years (Karunanayaka et al., 2007). These age-related connectivity changes have already shown in children at rest (Long et al., 2017). Taken together, a functional frontotemporal language comprehension network seems to be present in children. The left superior temporal cortex is initially involved, followed by the left inferior frontal cortex (Friederici, 2011; Skeide and Friederici, 2016), mediated by the left inferior parietal cortex (Catani et al., 2005; Makuuchi and Friederici, 2013; Obleser et al., 2007). Even though these studies provide initial insights into the developmental trajectory of the functional language comprehension network, the details are still missing, particularly in children between preschool and school-age (Enge et al., 2020). However, as preschool years are characterized by advancing development in the brain, as well as by steady changes in language comprehension ability (Dittmar et al., 2008; Gogtay et al., 2004; Lindner, 2003; Skeide and Friederici, 2016), further studies specifying the functional language comprehension network for this age period are necessary.

The above described maturation of the functional language networks relies heavily on the maturation of the structural networks, as has been consistently revealed in previous neuroanatomical studies. For instance, a long-range white matter connection between the left IFG and left posterior STG and superior temporal sulcus (STS) has been reported to emerge gradually with age and to relate to language abilities (Friederici, 2011; Skeide and Friederici, 2016). Moreover, brain regions of the gray matter linked to this fiber tract, e.g., the left IFG, left inferior parietal lobule (IPL), and left supramarginal gyrus, have also been observed to be associated with language skills in children and to change with development (Fengler et al., 2015; Lu et al., 2007; Qi et al., 2019a, 2019b; Richardson et al., 2010; Sowell et al., 2004). In general, myelination development parallels cortical growth, such as cortical surface expansion and thinning (Cafiero et al., 2018; Natu et al., 2019), gradually developing across frontal, temporal, and parietal regions (Brown et al., 2012; Cafiero et al., 2018; Raznahan et al., 2011; Tamnes et al., 2017), which are proposed to be associated with language comprehension (Roehrich-Gascon et al., 2015). Throughout early life, these anatomical changes accompany dynamic functional changes (Gilmore et al., 2018). More importantly, the available structural prerequisites, such as gradual maturation of the long-range structural language network in childhood, may also impact the development of language function. Taken together, the functional and structural language comprehension networks gradually develop across childhood and adolescence, and it has been suggested that the former depends on the latter to mutually influence children's language development. However, systematic studies simultaneously investigating the development of the functional network and its anatomical substrates are sparse in preschool and early school age children.

In the present study, we investigated the developmental trajectory of the functional language network and its cortical structures in a large cohort of young children between the ages of 4 and 9 years. We collected resting-state fMRI and T1-weighted structural MRI data and tested sentence comprehension abilities in a subgroup of children. Some of these children were re-invited one year and two years later, where we again assessed their sentence comprehension abilities. To provide a description of the development of the language network, we first investigated how the functional connectivity of the language network changes with age. Second, to examine whether functional connectivity mediates lan-

guage development, we assessed the correlation of functional connectivity of language-related ROIs with language abilities in children. Third, to determine that changes of the functional connectivity of the language network are accompanied by the maturation of involved brain structures, associations between functional connectivity and cortical morphology were assessed, namely cortical thickness and surface area. To specify the potential relation to language, the correlation between cortical structure maturation and the children's language abilities was further analyzed. Based on the observed, dynamic, regional, developmental trajectories in brain maturation (Gogtay et al., 2004; Petanjek et al., 2011), we expected functional connectivity changes across development, in particular between left inferior frontal regions and left temporoparietal regions. Further, the functional connectivity of the left IFG was expected to be associated with language abilities. Finally, we hypothesized that the development of functional connectivity would be associated with the cortical growth of the underlying brain regions.

2. Methods

2.1. Participants

A total of 221 children between the ages of 4 to 9 years, with complete structural and functional MRI scans collected across several projects by our group (Cafiero et al., 2018; Fengler et al., 2016; Kuhl et al., 2020; Skeide et al., 2016), were initially included in the current study. Forty-six children were excluded due to one of the following reasons: 1) bad image quality, e.g., large head motion in resting-state fMRI data ($N = 29$); 2) IQ below the normal range (i.e., $IQ < 85$, $N = 2$); and 3) left-handers ($N = 15$). The remaining 175 children, with an age range of 4.08 to 8.91 years (84 female, *mean* age = 6.13 years, $SD = 1.15$), entered the analyses. Handedness (*mean* = 77.02, $SD = 19.46$) was assessed using the modified version of the Edinburgh Handedness Inventory (Oldfield, 1971), which has been frequently used in previous studies of children and which assess handedness metrically (Wu et al., 2016). If participants receive a score of above 20, they can be considered as right-handed. Non-verbal IQ was available for 136 of the 175 children and was assessed either by using the German versions of the Kaufman Assessment Battery for Children ($N = 112$) (K-ABC, Kaufman and Kaufman 1983) or the Wechsler Preschool and Primary Scale of Intelligence ($N = 24$) (WPPSI-III, Petermann and Petermann 2011). Because of the standardization and the high correlation between the above-mentioned IQ tests (Kaufman, 2004), IQ scores from these two tests were taken as equivalent measures to indicate general cognitive ability. All included children with available IQ data had a non-verbal IQ above 85, with a mean IQ of 108.01 ($SD = 10.56$), ranging from 85 to 131, which is within and above the normal range (i.e., 85 to 115). For those children with missing IQ data, a typical IQ can be expected, as they were enrolled as typically developing children in one of our studies (Fengler et al., 2016). The distribution of age, language scores, and the inclusion procedure of participants are illustrated in Fig. 1. All participants were native German speakers, with no history of medical, psychiatric, or neurological disorders. Written informed consent was obtained from the legal guardian or parent of the children; while children gave verbal assent for participation before the experiments. The ethical review board of the University of Leipzig approved the study.

2.2. Behavioral language test

A standardized language test [Test zum Satzverstehen von Kindern, TSVK, (English: sentence comprehension test for children), Siegmüller et al., 2011] was administered assessing the general sentence comprehension abilities of a subgroup of participating children ($N = 100$, see Fig. 1). TSVK employs a picture matching task in which the child is auditorily presented with a sentence as well as three pictures. The child's task is to choose the picture that correctly matches the presented sentence. In total, the child is presented with 36 items that

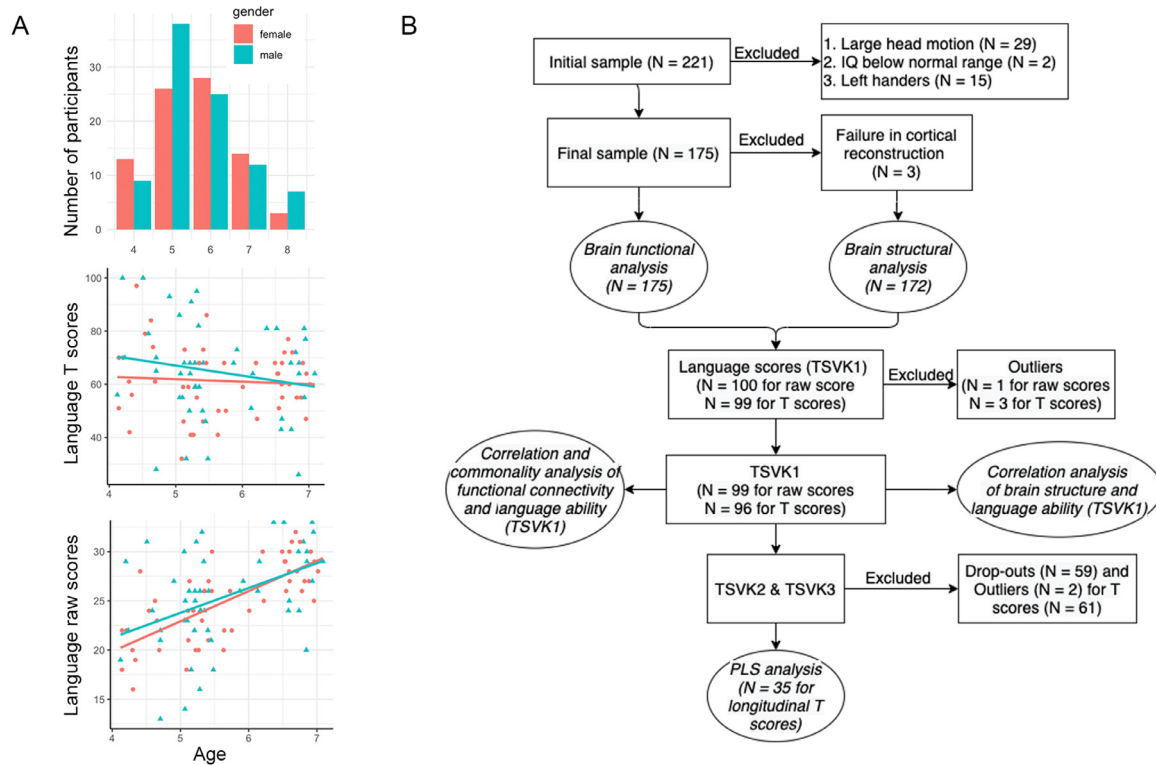


Fig. 1. Overview of participants. A) The number of participants and the distribution of language scores per year across the whole cohort. B) Flowchart for participant inclusion for each of the analyses. Italic indicates the sample included in the respective analysis. Regarding the brain data, children were excluded from the analysis because of large head motion (i.e., a max of 3 mm or 3°; 20% of the total volumes with framewise displacement larger than 0.3 mm or mean framewise displacement larger than 0.3 mm), below normal range IQ, and being left-handed. TSVK1, TSVK2, and TSVK3 (sentence comprehension test for children) denote the language tests performed at the first (when the brain scans were performed), second, and third testing time points. PLS stands for partial least squares.

vary in sentence complexity, which was manipulated by word order, tense, mode, clause number, pronoun type, and verb type. The number of correct responses (raw scores) gets summed and converted to norm-based standard scores. In this case, the standardized T scores with a *mean* of 50 and a *SD* of 10. The behavioral assessment was typically taken no more than 6 months apart from the MRI scan, with a *mean* interval of 0.02 (*SD* = 0.06, in years). The behavioral data were scanned for outliers using the criterion of 3 median absolute deviations from the median (Leys et al., 2013), resulting in 99 datasets for raw scores (*mean* = 25.18, *SD* = 4.44) and 96 datasets for T scores (*mean* = 62.93, *SD* = 15.62). Additional language scores were available for two follow-up assessments for a sub-group of 35 children after detecting outliers and removing drop-outs [*mean* = 62.69, *SD* = 16.83 at the first time point (*mean* age = 5.62, range = 5.07 - 6.96); *mean* = 60.37, *SD* = 14.09 at the second time point (*mean* age = 6.61, range = 6.06 - 7.79); and *mean* = 52.60, *SD* = 21.85 at the third time point (*mean* age = 7.73, range = 6.91 - 8.90) for T scores]. The detailed information regarding the sample inclusion for each analysis can be found in Fig. 1.

2.3. Data acquisition

Neuroimaging data were acquired with a 3.0 Tesla Siemens MRI scanner with a 12-channel head coil. Resting-state fMRI data were acquired with a $T2^*$ -weighted, gradient-echo, echo-planar imaging (EPI) sequence using the following parameters: TR = 2000 ms, TE = 30 ms, flip angle = 90°, slice thickness = 3 mm, FOV = 192 mm, matrix = 64 × 64, 28 slices, 100 volumes, spatial resolution = 3 × 3 × 3.99 mm³. During the resting-state data acquisition, children were instructed to lie down as still as possible, keep their eyes open and watch the visual presentation of a screensaver featuring a lava lamp. Of note, because young children are unable to tolerate longer resting-state scans during the wak-

ing state (Harms et al., 2018), the duration of the resting-state scan is relatively short, namely 3.3 min. However, a resting-state scan as brief as 3 min. can already show high inter-session reliability for functional homogeneity analyses and further shows high reliability with longer scans (Yan et al., 2013; Zuo et al., 2013). T1-weighted, magnetization-prepared, gradient-echo (MP-RAGE) images were acquired using the following parameters: TR = 1480 ms, TE = 3.46 ms, TI = 740 ms, flip angle = 10°, image matrix = 256 × 240, FOV = 256 × 240 mm², 128 sagittal slices, spatial resolution = 1 × 1 × 1.5 mm³. Before the formal MRI scanning, children were asked to participate in a mock scan to familiarize them with the experimental environment and procedures. This was to reduce head motion in formal scanning.

2.4. Data preprocessing

Before preprocessing, T1-weighted images were visually inspected for potential artifacts caused by head motion, to ensure that brain tissues could be well-differentiated. Cortical reconstruction and volumetric segmentation was performed using the FreeSurfer toolbox (version 7.1.0). The automatic processing procedure of FreeSurfer included skull stripping, gray matter segmentation, cortical surface model reconstruction, and a number of deformation procedures, including: surface inflation, registration to a spherical atlas, parcellation of the cerebral cortex, and creation of a variety of surface-based data (Dale et al., 1999; Fischl et al., 1999; Han et al., 2006). The reconstructed surfaces were visually inspected and manually edited for inaccuracies. Once surfaces were reconstructed, an array of anatomical measures, including cortical thickness and surface area, were then calculated at each vertex of the cortex. Cortical thickness was calculated as the closest distance from the pial surface to the white matter surface at each vertex (Fischl and Dale, 2002). The area was calculated at the pial level and represents the area of vertex

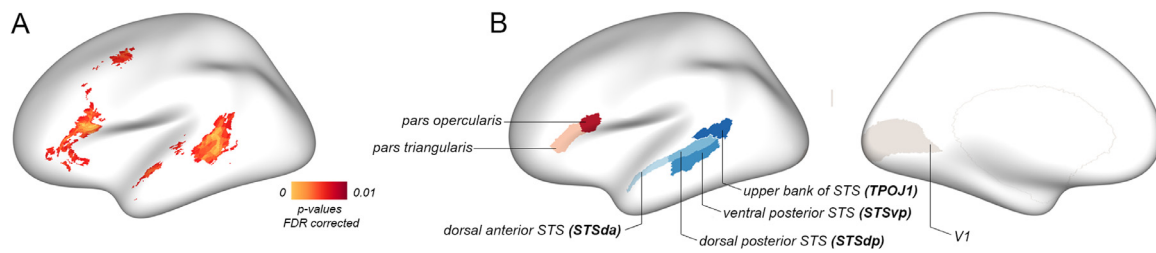


Fig. 2. Illustration of regions of interest (ROIs) that are relevant for language comprehension. A) Language comprehension network obtained based on the term “sentence comprehension” in the NeuroSynth Database. B) Six language-related ROIs, including pars opercularis and pars triangularis in the left inferior frontal gyrus, and STSVp, STSDp, TPOJ1 in the posterior left superior temporal regions, STSDa, together with a control ROI in left V1. STS: superior temporal sulcus; TPOJ: temporo-parieto-occipital junction.

on the gray matter surface, calculated as the average of the area of the tessellated triangles touching that vertex. The vertex-wise maps of individuals were aligned to the Freesurfer *fsaverage* surface-based template since it has been shown that using this template for children from ages 4 to 11 does not result in an age-associated bias (Ghosh et al., 2010). Finally, thickness and surface area maps were smoothed using a 25-mm FWHM Gaussian kernel. In total, 3 out of 175 children were discarded from the surface-based statistical analysis due to the failure of surface reconstruction or parcellation during image preprocessing (see Fig. 1).

In addition, all fMRI preprocessing was performed using FSL (version 5.0.11) and AFNI (version 19.1.05n). The functional preprocessing involved removing the first 3 volumes to allow for signal stabilization, slice timing correction, re-aligning to correct for head motion, and coregistration with T1 images. T1 images were segmented into gray matter (GM), white matter (WM), and cerebrospinal fluid (CSF) to create corresponding individual masks and then registered to the pediatric template in Montreal Neurological Institute (MNI) standard space (Fonov et al., 2011). The transformation of the functional images to the T1 image and subsequent transformation of the T1 image to the pediatric template were combined to register the functional images into MNI space at 3 mm. To account for motion, scanner-related, and physiological noise, 24 motion parameters (Friston et al., 1996) were regressed out, together with the first five principal components from WM and CSF tissues, using a component-based noise correction (Behzadi et al., 2007). This also involved detrending and variance normalization. Finally, residual images were bandpass filtered (0.009 - 0.08 Hz) and spatially smoothed with a 6 mm FWHM kernel.

Regarding head motion, children with a maximum of 3 mm or 3° were discarded from the analysis. Volume-to-volume framewise displacement (FD) was further quantified (Jenkinson et al., 2002; Power et al., 2012). Any child with 20% of the total volumes with FD larger than 0.3 mm or the mean FD larger than 0.3 mm was excluded, which is consistent with previous criteria used in studies of children (Gabard-Durnam et al., 2018; Long et al., 2017). This resulted in the exclusion of 29 children from the initial sample (also see above and Fig. 1). Although the mean FD was neither correlated with age (Spearman’s rank correlation, $\rho = -0.02$, $p = 0.835$), IQ ($\rho = -0.16$, $p = 0.067$), nor with language abilities ($\rho = -0.17$, $p = 0.097$ for *T* scores, and $\rho = -0.19$, $p = 0.055$ for raw scores; the correlation matrix of demographic and behavioral variables can be found in Table S1 in the supplements), it was included as a covariate of no interest in subsequent analyses.

2.5. Region-based functional connectivity analysis

To define language-related regions of interest (ROIs), we used the term “sentence comprehension” in NeuroSynth (Yarkoni et al., 2011) to identify the language network with the main focus on sentence comprehension. This resulted in a network consisting of two brain regions, the left IFG and the left superior temporal region (see Fig. 2), agreeing with previous studies (Friederici, 2011; Friederici et al., 2011). Specifically,

the left IFG included the pars opercularis and pars triangularis, making up the classical Broca’s area. The left superior temporal region included three subregions of the posterior superior temporal regions (STG/STSp), namely: ventral (STSVp), dorsal (STSDp), and the upper bank of STS (TPOJ1: temporo-parieto-occipital junction 1), as well as the dorsal anterior superior temporal sulcus (STSDa). In addition, as employed in previous studies, one control ROI, namely left V1, was selected to test the specificity of language (Xiao et al., 2016a). These 7 ROIs were then selected according to a commonly used multi-modal parcellation introduced by Glasser and colleagues (Glasser et al., 2016). For each ROI, its mean time series were correlated to time series of voxels within the whole brain to generate voxel-based *r*-maps for each individual. The *r*-maps were then converted to *z*-maps by subtracting the global mean and dividing by the standard deviation within the whole-brain mask. These will be referred to as functional connectivity (FC) maps in the following sections. This *z*-transformation increases the comparability and reliability of the whole brain voxel-wise metrics across participants and does not affect the topography of centrality measures (Buckner et al., 2009; Zuo et al., 2010).

2.6. Statistical analysis

A one-sample *t*-test was conducted for the resulting FC maps per ROI to identify significant FCs that are larger or smaller than zero. Given the evidence of different connectivity profiles, both structurally and functionally, of the subdivisions of the left IFG (Amunts et al., 2003; Friederici, 2011; Xiang et al., 2010), we further compared the FC maps of the left pars opercularis and pars triangularis using a paired two-sample *t*-test. Next, linear regression analysis was performed to examine linear and nonlinear (i.e., quadratic) associations between FC maps and age. For all analyses, sex, head motion, and the continuous variable handedness (see Methods 2.1 for details) were considered as covariates of no interest to control for potential influences. For non-age-related analysis, age was additionally taken as a covariate of no interest. If not otherwise specified, the statistical maps were corrected for multiple comparisons using Gaussian random field theory (Nichols and Hayasaka, 2003) at a voxel-wise *p*-value of 0.001 and a cluster-wise *p*-value of 0.05. For a better visual comparison with structural MRI results, the volume result was projected on an averaged mid-surface template.

In a next step, FC that was significantly correlated with age was used for subsequent analyses to investigate whether it associates with language development. First, the correlation was assessed between age-related FC and language raw scores for our subgroup of children with one assessment of language scores (i.e., $N = 99$ for raw scores, details see Fig. 1), partialling out the above-mentioned covariates of no interest. Next, a commonality analysis was conducted to examine the relationship between age, FC, and language raw scores. Specifically, age and FC were included as predictors of the dependent variable language performance using the *yhat* package (Nimon et al., 2008) implemented in R. Commonality analysis decomposes the contributions of several, possibly intercorrelated, linear predictors into unique effects and indicates how

much variance is uniquely accounted for by single predictors and how much is shared (Ray-Mukherjee et al., 2014). Three variance partitions were obtained: the variance uniquely explained by 1) age, 2) FC, and the variance explained jointly by 3) age and FC. To further verify the contribution of general cognitive abilities, IQ was additionally included in the analysis. We then performed bootstrapping analysis with 1000 iterations to compute 95% confidence intervals (CIs) around the commonalities. These CIs can be used to identify whether the contribution of the predictors (i.e., age and FC) to the explained variance in the dependent variable (i.e., language ability) is different from zero (Prunier et al., 2015).

To further investigate the association between FC and language abilities, independent of age, we took a conventional univariate approach, assessing correlation between the FC maps of each ROI and children's age-standardized language scores, i.e., T scores ($N = 96$, Fig. 1). Moreover, to fully examine the potential time-varying brain-behavior relationship between ROI-based functional connectivity and language performance, an exploratory, partial least squares correlation analysis (PLS, McIntosh et al., 1996) was performed using available longitudinally language T scores ($N = 35$, details see Fig. 1). This approach has been frequently used in recent neuroimaging studies, capturing multivariate patterns of correlation between behavior and brain (Kebets et al., 2019; Zöllner et al., 2017). As mentioned above, PLS is a multivariate statistical technique that maximizes the covariance between two sets of variables by extracting latent components (LCs). It is optimal for linear combinations of the variables, in comparison to the conventional univariate approach (for more details, see Krishnan et al., 2011; McIntosh and Lobaugh, 2004; McIntosh and Mišić, 2013). All analyses were conducted using the *my-pls* toolbox (<https://github.com/danizoeller/myPLS>) implemented in Matlab. Before PLS analysis, covariates of no interest, namely sex, handedness, and head motion were regressed out from the original data. Data were then transformed to z-scores across all subjects. The resulting FC data matrix (subjects by FCs) and behavioral data matrix (subjects by language scores) were taken as inputs for the PLS analysis. PLS computes the strongest multivariate correlation between the two matrices by deriving LCs. Each LC is characterized by a distinct FC pattern (i.e., brain salience) and a distinct behavioral pattern (i.e., behavioral salience). The brain salience indicates the contribution of each voxel to the brain-behavioral covariance of the LC while the behavioral salience represents the contribution of each behavioral measurement to the LC. By linearly projecting the original brain and behavioral measurements of each subject onto their respective salience, we also obtained an individual-specific PLS brain score and PLS behavioral score for each LC respectively. The statistical significance of each LC was determined with a (1000 iteration) permutation test (Kebets et al., 2019; Zöllner et al., 2019). P -values were corrected for multiple comparisons using a false discovery rate (FDR) correction of $q < 0.05$. For each LC, we computed correlations (i.e., brain loadings) between the original brain FC pattern and PLS brain scores, as well as correlations (i.e., behavioral loadings) between the original behavioral measurements and PLS behavioral scores. A high correlation for a specific behavioral measurement for a given LC would indicate greater contribution of the behavioral measurement to the brain-behavioral covariance for the LC. Likewise, a high correlation for specific brain measures (i.e., voxels functionally connected with the ROIs) for a given LC would indicate greater contribution of the voxel to the brain-behavioral covariance for the LC. The CIs for these correlations were estimated by bootstrapping (500 iterations) that randomly resampled subjects with replacement to evaluate the robustness of brain and behavior loadings. The bootstrapping distribution was used to estimate the standard error for each correlation. Z -scores were calculated by dividing each correlation coefficient by its estimated standard deviation. The z -scores were converted to p -values and corrected for multiple comparisons ($q < 0.05$, FDR-corrected) (Kebets et al., 2019; Zöllner et al., 2019).

Finally, we examined whether brain function is constrained by brain structure, that is, whether age-related FC interacts with the maturation

of brain structure (i.e. surface area and cortical thickness). The correlation was assessed between the structural indices, of the two age-related functionally connected nodes (i.e., the left pars triangularis and the left IPL/STSp), and the corresponding FC strength. Further, we also tested the correlation of the structural measurements and language abilities (i.e., T scores) to determine whether the local morphology was relevant for language abilities. The same analysis was repeated across the entire brain, at the vertex level using the *surfstat* toolbox (<https://www.math.mcgill.ca/keith/surfstat/>) implemented in Matlab, to verify whether the observed association was specific to language-related ROIs. Of note, covariates of no interest, namely sex, handedness, total brain volume, and age were included in the analysis. All surface-based results were thresholded with a cluster-forming threshold of p -value < 0.005 at a cluster level of p -value < 0.05 corrected for multiple comparisons based on random field theory (Worsley et al., 1999).

3. Results

3.1. Functional connectivity of language-related ROIs

Inferior frontal ROIs. We first examined the FC of language-related ROIs in the inferior frontal regions, namely the pars opercularis and pars triangularis. The left pars opercularis was positively correlated with bilateral IFG, STG, middle temporal gyrus (MTG), and the left superior and middle frontal gyrus, insula, and IPL. It was also negatively connected with the bilateral posterior superior parietal gyrus and precuneus, and the right superior frontal gyrus. A very similar pattern was observed for the left pars triangularis (see Fig. S1 in the supplements). Despite the similar FC pattern for these two subdivisions of the left IFG, different anatomical and functional connectivity profiles have been shown (Amunts et al., 2003; Friederici, 2011; Xiang et al., 2010). Therefore, we further examined the difference between the FC maps of these two IFG ROIs and found that the left pars opercularis was more strongly connected with the bilateral dorsal IFG, MFG, and the left precentral gyrus, middle STG, and IPL than the left pars triangularis. The left pars triangularis in comparison to the left pars opercularis was more connected with the ventral IFG, insula, MTG, anterior temporal areas, and temporal pole bilaterally (see Fig. 3, $p < 0.05$, GRF-corrected; cluster with positive Z score: $Z_{\text{mean}} = 5.54$, cohen's $d = 0.84$, CI: 0.54 - 1.13; cluster with negative Z score: $Z_{\text{mean}} = -5.49$, cohen's $d = -0.83$, CI: -1.13 - -0.53).

Superior temporal ROIs. The left STSdp was positively connected with most parts of bilateral superior and middle temporal regions, extending to the left IPL, and bilateral IFG and left precentral gyrus. It was also negatively connected with the bilateral posterior parietal, superior frontal, and precuneus regions. The left STSvp and TPOJ1 showed similar functional connectivity patterns as the left STSdp, except that these two ROIs showed more positive connectivity with the bilateral IPL and lateral occipital regions. Regarding the left STSda, positive connectivity with most of the bilateral temporal regions and inferior frontal regions, as well as a negative connectivity with the right middle frontal, bilateral superior frontal regions, and posterior inferior and superior parietal regions were revealed (see Fig. S1 in the supplements).

3.2. The role of age in brain functional connectivity and language performance

3.2.1. Age-related differences in the functional connectivity of language-related ROIs

The FC between the left pars triangularis and left IPL extending to the left STG/STSp (referred to as $FC_{\text{tri-IPL/STSp}}$ in the following) was positively correlated with age ($p < 0.05$, GRF-corrected, $Z_{\text{mean}} = 3.57$, cohen's $d = 0.54$, CI: 0.24 - 0.84, see Fig. 4). Further, the FC between the left TPOJ1 and the right IPL (referred to as $FC_{\text{TPOJ1-IPL}}$ in the following) was positively associated with age ($p < 0.05$, GRF-corrected, $Z_{\text{mean}} = 3.71$, cohen's $d = 0.56$, CI: 0.26 - 0.86, see Fig. 4). No linear

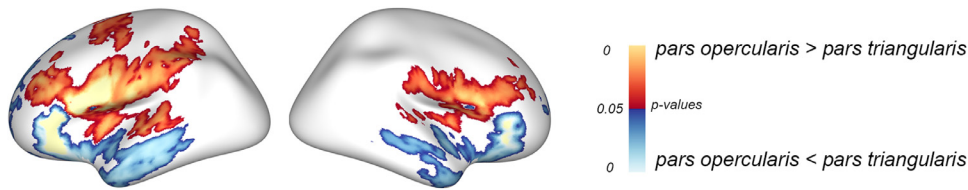


Fig. 3. Comparison of the functional connectivity between the left pars opercularis and the left pars triangularis. Group-level maps were thresholded with a cluster-forming threshold of $p < 0.001$ at a cluster level of $p < 0.05$ (GRF-corrected).

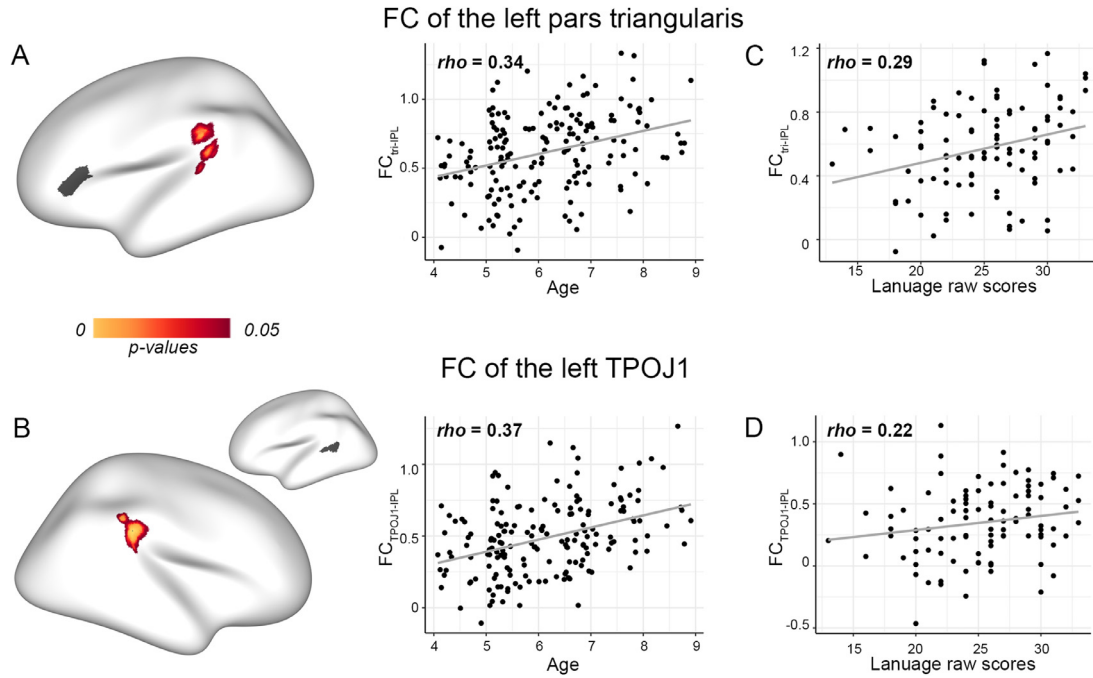


Fig. 4. Age-related differences in functional connectivity of the language-related ROIs. Linear associations showing an increase in functional connectivity of left pars triangularis (A) and left TPOJ1 (B) with age. Associations between age-related functional connectivity of left pars triangularis (C) and left TPOJ1 (D) and raw scores of the language comprehension test. Note, dark gray colored brain regions in A and B denote the language-related ROIs, namely the left pars triangularis and TPOJ1, respectively.

age effect was found for other language-related ROIs. The significant functional connectivity was further examined in the following analyses. Given the possibility of the non-linear association, we additionally examined a non-linear quadratic age effect on FC for each ROI. A quadratic age effect was found for the FC between the left pars opercularis and the right inferior occipital gyrus (IOG), and the FC between the left STSdp and the right IOG ($p < 0.05$, GRF-corrected, Fig. S2 in the supplements), suggesting that the FC between the left IFG/STSdp and the right IOG first decreases and then increases with age.

3.2.2. Age-related functional connectivity mediates language performance

We then examined if the significant age-related FC mediates language performance. Analyses showed that raw scores were associated with age-related FC, namely $FC_{tri-IPL/STSp}$ ($\rho = 0.29$, $p = 0.004$, $CI: 0.10 - 0.46$, Fig. 4A) and $FC_{TPOJ1-IPL}$ ($\rho = 0.22$, $p = 0.026$, $CI: 0.03 - 0.40$, Fig. 4B). The correlation with language raw scores remained when controlling for sex, handedness, head motion, and IQ in the $FC_{tri-IPL/STSp}$ ($\rho = 0.30$, $p = 0.003$, $CI: 0.11 - 0.47$), but was no longer significant in the $FC_{TPOJ1-IPL}$ ($\rho = 0.16$, $p = 0.134$, $CI: -0.04 - 0.35$). This finding showed that children who are better with language have higher FC between the left IPL/STSp and the left IFG and that this association is likely influenced by age.

To further explore the relationship between age, FC, and language ability, a commonality analysis was conducted to examine to which extent the predictors, namely age and FC (e.g., $FC_{tri-IPL/STSp}$), uniquely and commonly contributed to language performance. The result showed that $FC_{tri-IPL/STSp}$ and age accounted for 32.72% of the language performance

variance (i.e., TSVK variance). Age had the largest unique contribution (24.47%, $CI: 0.11 - 0.38$) beyond that of $FC_{tri-IPL/STSp}$ (1.40%, $CI: 0.00 - 0.07$). Despite the smaller contribution of $FC_{tri-IPL/STSp}$, variance shared by $FC_{tri-IPL/STSp}$ and age explained 6.85% ($CI: 0.01 - 0.16$) of the language performance variance. We also examined the contribution of age and $FC_{TPOJ1-IPL}$ to explaining language performance variability but did not find significant effects. Thus, only the $FC_{tri-IPL/STSp}$ was used for the following analysis. To investigate how general cognitive abilities, together with FC and age, account for language performance, IQ was additionally included in the model. Age, IQ, and $FC_{tri-IPL/STSp}$ showed significant unique contributions to the variance of language performance (19.24%, $CI: 0.08 - 0.32$ for age; 6.67%, $CI: 0.01 - 0.17$ for IQ; 2.11%, $CI: 0.01 - 0.08$ for $FC_{tri-IPL/STSp}$) together with the common contribution of age and $FC_{tri-IPL/STSp}$ (7.16%, $CI: 0.02 - 0.15$). These results suggest that although age and IQ contributed most, the FC differences between the left pars triangularis and the left IPL/STSp could still uniquely explain variance in children's language abilities.

3.3. The role of language performance in functional connectivity

We continued to investigate how FC covaries with language abilities, independent of age. We first examined the correlation between FC of the ROIs and age-standardized language T scores (which should effectively nullify age effects) from the first testing time point. No significant effect was found. To additionally investigate the potential association between the brain and behavioral measures, and to make full use of our available data, we performed an exploratory multivariate PLS analysis. This max-

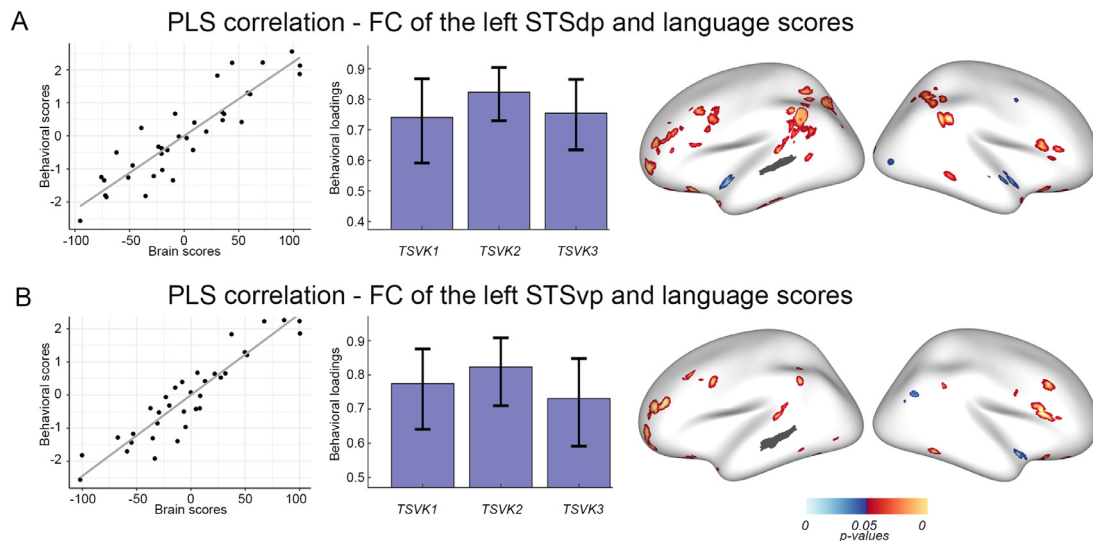


Fig. 5. Significant LC of PLS analysis for functional connectivity of the left STSdp (A) and the left STSvp (B) and language scores. The left panel illustrates the correlation between PLS brain scores and PLS behavioral scores; the middle panel illustrates the significant correlation between PLS behavioral scores and language tests; the right panel illustrates the significant correlation between PLS brain scores and functional connectivity of the left STSdp (A) and the left STSvp (B) ($q < 0.05$, FDR-corrected). Warm colors denote positive correlations, meaning that higher functional connectivity corresponds to superior language abilities, while cool colors denote negative correlation, meaning that higher functional connectivity corresponds to weaker language abilities. Note, TSVK1, TSVK2, TSVK3 denote the language comprehension test at the first (mean age = 5.61), second (mean age = 6.61), and third (mean age = 7.73) testing time points. Dark gray colored brain regions in the right panel denote the language-related ROIs, namely the dorsal and ventral part of the left posterior STS, left STSdp (A), and the left STSvp (B), compare Fig. 2.

minimizes the covariance between two sets of variables by extracting latent components (LC). More specifically, we used the longitudinal language T scores from three testing time points ($N = 35$, see Fig. 1) and the FC of the language-related ROIs at each voxel.

Our first PLS results showed one significant LC ($p_{\text{uncorrected}} < 0.01$, $q < 0.05$, FDR-corrected) for the association between the FC of the left STSdp and language performance. More specifically, the surviving LC accounted for 67.28% of brain-behavior covariance, with a significant correlation ($r = 0.90$, $p < 0.001$) between the PLS brain score and PLS behavioral score (see Fig. 5A, left panel). The PLS behavioral score, which indicates the contribution of each behavioral measurement (i.e., three language scores) for this LC, was positively correlated with all three language T scores (Fig. 5A, middle panel), suggesting that a greater PLS behavioral score was associated with greater language performance over time. The PLS brain score, which indicates the contribution of the ROI-based FC at each voxel for this LC, was positively associated with an increase in FC between the left STSdp and the bilateral IFG and IPL (Fig. 5A, right panel). This PLS result further suggests that stronger FC between the left STSdp and the bilateral IFG and IPL covaries with higher language performance in children over time. Negative correlations were found between PLS brain scores and FC of the left STSdp in the bilateral anterior superior temporal regions and the right occipital regions. This suggests that a reduction in FC between the left STSdp and bilateral anterior temporal and right occipital regions was associated with an increase in children's language performance over time. When baseline age (i.e., age at the first testing time point) was additionally controlled for ($p_{\text{uncorrected}} < 0.02$, $q < 0.05$, FDR-corrected), results showed a similar pattern.

In addition, we also found one significant LC ($p_{\text{uncorrected}} < 0.01$, $q < 0.05$, FDR-corrected) for the association between the FC of the left STSvp and language performance. The surviving LC accounted for 67.90% of brain-behavior covariance, with a significant correlation ($r = 0.93$, $p < 0.001$) between the PLS brain score and PLS behavioral score (see Fig. 5B, left panel). The PLS behavioral score was positively correlated with all language measurements (i.e. three language T scores, Fig. 5B, middle panel), indicating that a greater PLS behavioral score was associated with better language performance in children over time. In addition, a greater PLS brain score was associated with increased FC

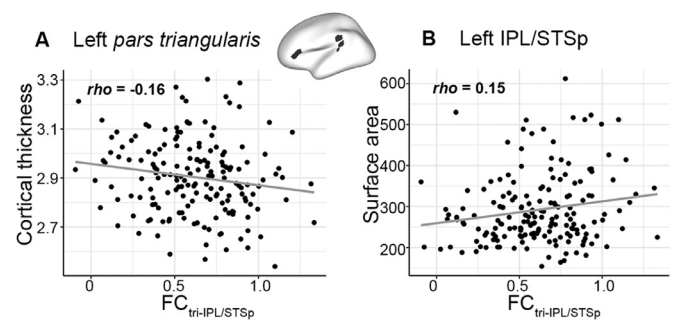


Fig. 6. Association between $FC_{\text{tri-IPL/STSp}}$ and the cortical measurements of the two nodes. A. Cortical thickness of the left pars triangularis was significantly correlated with $FC_{\text{tri-IPL/STSp}}$. B. Surface area of the left IPL/STSp was significantly correlated with $FC_{\text{tri-IPL/STSp}}$. The middle brain map denotes the two nodes (i.e., the left pars triangularis and the left IPL/STSp of the $FC_{\text{tri-IPL/STSp}}$).

between the left STSvp and the bilateral IFG, MFG, and the left IPL (Fig. 5B, right panel). The significant correlation between PLS brain and PLS behavioral scores further suggests that increased FC between the left STSvp and the bilateral IFG, MFG, and the left IPL was associated with better language performance in children. A marginally significant effect was found when baseline age was additionally controlled for ($p_{\text{uncorrected}} = 0.02$, $q = 0.06$, FDR-corrected).

3.4. The association between language-related cortical structural growth and functional connectivity

We also investigated how age-related functional connectivity is associated with the brain's cortical structural differences. The cortical measurements of the two nodes of the age-related $FC_{\text{tri-IPL/STSp}}$, namely the left pars triangularis and the left IPL/STSp, were correlated with the age-related functional connectivity. Analyses showed that greater $FC_{\text{tri-IPL/STSp}}$ was associated with thinner cortical thickness in the left pars triangularis ($\rho = -0.16$, $p = 0.033$, $CI: -0.31 - -0.01$, see Fig. 6A) and with greater surface area in the left IPL/STSp ($\rho = 0.15$, $p = 0.045$,

CI: 0.01 - 0.30, see Fig. 6B). These results suggest that stronger FC between the left pars triangularis and the left IPL/STSp is likely attributable to the maturational status of the corresponding brain structures.

Moreover, we examined whether the cortical measurements of the two nodes were associated with language performance (i.e., T scores). No significant correlation was found between the cortical thickness and surface area of the left pars triangularis of the left IPL/STSp and language T scores. Cortical thickness of the left pars triangularis was however, correlated with children's language raw scores ($\rho = -0.26$, $p = 0.009$, CI: $-0.43 - -0.07$). This suggests that the association between the cortical thickness of the left pars triangularis and language performance was mostly driven by age, which might not be specific to language. To further investigate whether the association between children's abilities and cortical structure is specific to the left IFG, we further performed a whole-brain analysis. We found a significant positive correlation between surface area and language T scores ($p < 0.05$, FWE-corrected, Fig. S3 in the supplements) in the left prefrontal cortex, including the left IFG, MFG, and SFG. Age, sex, handedness, and total brain volume was controlled for in this analysis. The effect remained ($p < 0.05$, FWE-corrected) when IQ was additionally included as a covariate of no interest, with the significant cluster contracting to more dorsal parts of the left prefrontal cortex. Thus, although the association between cortical thickness of the left IFG and language was mostly driven by age, greater surface area of the left prefrontal cortex was associated with superior language abilities. Together, our findings indicate that cortical structure, in particular the surface area of the left prefrontal cortex, is associated with brain function and language abilities in children.

3.5. Functional connectivity of non-language related ROIs

To investigate the specificity of our findings for language abilities and related brain regions, we performed all the analyses for the non-language related ROI, namely left V1 (Fig. S4 in the supplements). First, the FC between left V1 and the surrounding areas of the ROI, including the left V2 and V3, and the contralateral homologous regions, including the right V1, V2, V3, and V4, was functionally negatively correlated with age ($p < 0.05$, GRF-corrected, Fig. S4B). Second, neither the language score from the first testing time point (i.e., T scores at the same brain testing time point) in the conventional correlation analysis ($p > 0.05$, GRF-corrected) nor the longitudinal language scores (i.e., T scores of three testing time points) in the exploratory PLS analysis significantly coupled with the FC of left V1 ($p_{\text{uncorrected}} > 0.05$). This result suggests a language-specific functional connectivity development in children in the language-related brain regions.

4. Discussion

To gain a better understanding of the emergence of the functional network underlying language comprehension, during language development, the present study focused on the development of functional connectivity (FC) of core language regions and the extent to which changes relate to language abilities and the structural maturation of the brain. We examined the functional connectivity of subregions of the left IFG and the left STG/STS in a large cohort of children between 4 and 9 years old, a developmental time window characterized by steady development in language capacities. We found significant age-related differences in the FC of the pars triangularis of the left IFG, which was also correlated with language comprehension abilities in children. Furthermore, greater language abilities, independent of age, were associated with stronger FC between the left STSp and bilateral prefrontal cortex and inferior parietal regions. Finally, by examining the cortical structure in association with the functional connectivity, a more mature cortical structure, that is thinner cortical thickness in the left IFG and greater surface area in the left IPL/STSp, was revealed to be associated with stronger FCs between these regions. More importantly, this more mature structural pattern of

the left IFG was found to be associated with better language abilities in children.

4.1. The functional connectivity of the language-related ROIs in children

Using subdivisions of the left IFG or left STG/STSp as seed regions has revealed a fronto-temporal language comprehension network, including the perisylvian language regions like the left IFG and bilateral STG and MTG. This is in line with the consistently reported language comprehension network, in particular for children (Enge et al., 2020; Weiss-Croft and Baldeweg, 2015). In addition, the proposed functional and anatomical specialization between the subdivisions of the left IFG in previous task-based functional and anatomical neuroimaging studies (Amunts et al., 2003; Skeide et al., 2014) has also been observed in the present study. Specifically, when comparing the functional connectivity of the left pars triangularis and pars opercularis, we showed that the left pars opercularis was connected with bilateral dorsal IFG, MFG, precentral gyrus, STG, and IPL, while the left pars triangularis was mainly connected with bilateral ventral IFG, insula, and anterior temporal regions. This is in line with a previous task-based study of children where different functional connectivity strengths were observed when seeding from the left pars triangularis and the left pars opercularis during auditorily presented sentences (Vissienon et al., 2017). This finding is also in agreement with previous resting-state functional connectivity studies in adults, where different functional topographic patterns for the left frontal, temporal, and parietal regions were revealed when seeding from the subregions of the left IFG (Xiang et al., 2010). Corresponding to the different maturational trajectory of the white matter connectivity of the left IFG (Brauer et al., 2013; Perani et al., 2011), the different functional connectivity patterns of the subregions of the left IFG might be associated with the structural prerequisites, which will be discussed in detail below. Thus, we extend previous findings by suggesting that different functional connectivity profiles of the subregions of the left IFG are already present in young children.

4.2. The developing language comprehension network in children

We found two functional connections that increased with age: an intra-hemispheric connection between left pars triangularis and left temporal-parietal regions and an inter-hemispheric connection between left TPOJ1 and right IPL. This finding is compatible with previous resting-state fMRI studies, showing age-related local and global connectivity increases in middle and inferior frontal and inferior parietal areas in children between the ages of 2 and 7 years (Long et al., 2017). Similarly, increases in the asymmetry of functional connectivity with the left pars triangularis (Reynolds et al., 2019). Moreover, our finding is in line with previous studies showing that adults have stronger left-sided, long-range connectivity between the IFG and STGp and IPL, compared to preschoolers (Friederici et al., 2011; Xiao et al., 2016a). Of note, the presently reported functional connectivity increases, between the left pars triangularis and the left IPL/STSp, are slightly different from the findings reported in a previous task-based fMRI review. In that report, age-related increases were mainly found in the receptive sentence comprehension network in bilateral temporal regions during development (Weiss-Croft and Baldeweg, 2015). This discrepancy might be attributed to different language modalities, age ranges (early versus late childhood), and/or task states. No significant associations between FC and age were obtained when examining control ROIs. This further indicates that the observed effects reflect functional maturation specifically of language networks, rather than a general developmental trend. Furthermore, the significant age effect was only observed for the pars triangularis of the left IFG, and not the pars opercularis. As discussed above, the difference between these subregions of the left IFG could be associated with age, particularly the relatively immature left pars opercularis in children. Furthermore, activation peaks have commonly been observed in the left pars triangularis in children, in contrast to the left

pars opercularis in adults, when comprehending sentences (Brauer et al., 2011; Enge et al., 2020; Skeide et al., 2014; Wu et al., 2016). Consistent with those studies, our finding further emphasizes the crucial role that the left pars triangularis plays in early language acquisition.

Furthermore, and in line with our results that the left IFG was strongly connected with left temporal-parietal regions (STS/STGp and IPL). Left STS/STGp has been suggested to subserve the integration of syntactic and semantic information. Left IPL, which is commonly assumed to play a critical role in verbal working memory (Novais-Santos et al., 2007; Owen et al., 2005), has also been suggested to be a part of the language comprehension network (Friederici, 2011), particularly in children (Brauer and Friederici, 2007; Fengler et al., 2016; Knoll et al., 2012). Specifically, the left IPL has been proposed to subserve verbal working memory in sentence and complex linguistic processing (Makuuchi and Friederici, 2013; Meyer et al., 2012; Novais-Santos et al., 2007; Xu et al., 2005). For example, activation of the temporo-parietal cortex has been associated with storage distance in children and adults, and was also predicted by working memory performance in young children during sentence processing (Fengler et al., 2016; Määttä et al., 2014; Meyer et al., 2012; Montgomery et al., 2008; Weighall and Altmann, 2011; Yeatman et al., 2010). Further, a previous study in adults has shown that a hierarchical functional connectivity between the working memory (e.g., IPL) and core language systems (e.g., IFG) increases with sentence processing loads (Makuuchi and Friederici, 2013). Thus, when also considering our results, a progressive maturation of the hierarchical language system during language acquisition could be suggested. Further, the development of the language system would seem to be constrained by the development of the working memory system. This is particularly the case as it has been proposed that the left pars triangularis may also contribute to sentence comprehension in terms of syntactic working memory in adults (Fiebach et al., 2005).

We also found inter-hemispheric FC increases between the left TPOJ1 and the right IPL. This is in line with previous studies suggesting that the right hemisphere is likely to support the immature language processing of the left hemisphere in early childhood (Holland et al., 2007; Xiao et al., 2016a). Together, the left pars triangularis, which is particularly crucial for children, and the left temporoparietal region were strongly connected, and this connectivity shows a linear increase with age in young children.

4.3. The association between brain and language abilities

To investigate whether an increase in functional connectivity associates with language abilities, we assessed the correlation of the age-related functional connectivity with language scores. A positive correlation was observed with raw language scores, but not age-standardized *T* scores. This finding, as expected, indicates that the brain-behavior association is mainly driven by age, given that age not only uniquely explains the language ability increase but also does so jointly with the functional connectivity (e.g., between the left pars triangularis and the left IPL/STSp). More importantly, independent from age, the specificity of the functional connectivity for language abilities was demonstrated by examining its association with age-standardized language *T* scores. Despite the non-significant results using the conventional correlational approach (of FC and language *T* scores), significant associations were found with the exploratory multivariate PLS analysis. Specifically, higher longitudinal language *T* scores were associated with a stronger coupling of the left STSdp with the bilateral IFG and IPL and a stronger coupling of the left STSvp with the bilateral prefrontal areas and IPL. This suggests that children with superior language abilities, over time and independent from age, have greater functional connectivity in the bilateral frontotemporal and temporoparietal language networks. Our results add to previous findings, indicating that better language skills were associated with stronger connectivity within the language comprehension network in children (Fengler et al., 2016; Knoll et al., 2012; Nuñez et al., 2011; Skeide et al., 2016; Wu et al., 2016; Xiao et al.,

2016a, 2016b; Yeatman et al., 2010). It should be noted that our results have demonstrated a correlation between brain and language performance but cannot confirm it causally. However, studies with aphasic patients have shown that damage to the left arcuate fasciculus is strongly associated with syntactic deficits (Galantucci et al., 2011; Wilson et al., 2011), which might imply a causal connection. Therefore, we argue that the functional connectivity of the bilateral prefrontal cortex with the bilateral temporoparietal regions, increases with language abilities regardless of age.

To rule out the possibility that our effects were more generally related to development, the functional connectivity of a control ROI, namely the left V1, was also investigated. In line with previous studies (Qi et al., 2019a; Xiao et al., 2016a), neither age nor language abilities were significantly associated with the connectivity of the control ROI. This suggests the functional connectivity and age-related findings are specific to language development, rather than a general trend in brain maturation and/or general changes in cognition. Taken together, we suggest that the bilateral prefrontal and temporoparietal regions become more functionally connected across development, seemingly as a function of improving language abilities in parallel with age.

4.4. The association between the brain structure and function

As briefly discussed above, dynamic brain development and its associated functions might be constrained by the maturation of the underlying structure (Gilmore et al., 2018; Skeide et al., 2016). In line with this claim, our findings show that the functional connectivity strength between the left pars triangularis and the left IPL/STSp was correlated with the cortical thickness of the left pars triangularis as well as the surface area of the left IPL/STSp. This extends previous findings of associations between the functional complexity of the left inferior frontal and temporoparietal regions and their gray matter volume (Fengler et al., 2016). It is also consistent with associations between activation intensity during syntactic processing and cortical thickness of the IFG (although observed in the right hemisphere) (Nuñez et al., 2011). Cortical thinning and surface expansion have been proposed to be linked with certain processes, such as synaptic pruning, myelination, and dendritic arborization (Brown and Jernigan, 2012; Hill et al., 2010; Petanjek et al., 2011). Thus, we conclude that the functional connectivity increases of the left frontoparietal regions are associated with one of these maturation mechanisms of the underlying gray matter. The maturation of brain structure provides the basis for the establishment of cognitive abilities and optimal acquisition of learning opportunities during development.

To further elucidate whether brain structure is related to language, we tested the correlation of our structural indices of the left pars triangularis and IPL/STSp with language scores. Cortical thickness of the left pars triangularis was indeed negatively correlated with language raw scores, but not with *T* scores. This suggests that although greater cortical thinning (a more mature pattern during development) in the left pars triangularis was associated with greater language abilities, this association is most likely driven by age and might not be specific to language. Further, we examined the relationship between language scores and the brain structure across the entire brain to test whether such correlations were specific to our language-related ROIs. A positive correlation with language *T* scores was found for surface area in the left prefrontal cortex, including the left IFG and MFG. That is, the association of language scores with cortical thickness of the left prefrontal cortex seems to depend on age, while the association with surface area appears independent of age. More importantly, our findings are in line with previous studies showing that language abilities are associated with gray matter measures in the left IFG, MFG, and IPL in children (Fengler et al., 2016; Qi et al., 2019b; Sowell et al., 2004). Specifically, the left prefrontal cortex, including the left IFG and MFG, undergoes a prolonged maturation, which is possibly related to environmental impacts on a sophisticated language system (Petanjek et al., 2011; Thompson-schill et al., 2009). Taken together, the maturation of brain structure, in particular the left

prefrontal cortex, seems to provide the basis for the establishment of the brain functions related to sentence processing in children.

4.5. Limitation and future directions

It is important to acknowledge a few limitations of the present study. First, due to the effort and difficulty in data acquisition, particularly in children younger than 7 years of age (Harms et al., 2018), the scan duration of the resting-state data of the present study is short (i.e., 3.3 min). Although evidence has indicated that scan duration of 3 min already shows high reliability for resting-state fMRI measures (Yan et al., 2013; Zuo et al., 2013), longer scans or short scans with multiple runs are warranted in future studies with children for a more stable estimation (Harms et al., 2018; Marek et al., 2019; Van Dijk et al., 2010). Second, we used cross-sectional data to investigate the developmental changes of the functional connectivity of the language network. This should be more sufficiently investigated by employing a longitudinal design in future studies. Third, due to the specific interest in early language acquisition, our sample included children from 4 to 9 years of age. However, from the perspective of language development, a larger age range, extending to early adolescence (i.e., 9 to 11 years) should also be included. This is particularly true when considering that the maturation of the pars opercularis of the left IFG progresses into early adolescence (Skeide et al., 2014; Skeide and Friederici, 2016). This might also explain the non-significant effect for the left pars opercularis in the present study. Moreover, although the multivariate approach, such as PLS, outperforms univariate techniques in brain-behavior correlations and provides some benefit with smaller sample sizes (Grady et al., 2021; Lukic et al., 2002), we still need to point out that the sample size used for the PLS analysis was small ($N = 35$). Thus, the exploratory finding reported in the present study should be treated with caution and needs to be verified in a larger sample. Finally, we investigated only gray matter with respect to functional connectivity. Future studies analyzing white matter connections may provide a more direct understanding of brain function and structure couplings during language development.

5. Conclusion

In the present study, we have demonstrated functional connectivity increases of language-related regions in a large cohort of children between the ages of 4 to 9 years. We have shown that functional connectivity between the left pars triangularis and left IPL, extending to the left STSp, increases with age, and that this connectivity coupled with age is associated with children's language abilities. This age-related functional connectivity between the left IFG and the left IPL/STSp was further associated with a more mature structural pattern, that is, greater cortical thinning in the left IFG and greater surface area in the left IPL/STSp, which was also related to language abilities in children. Moreover, we found greater language abilities to be associated with stronger functional connectivity between the left STSp and the more distributed bilateral prefrontal and temporoparietal regions, when age was controlled for by using age-standardized T scores. By merging functional, structural, and behavioral measures, we provide further insights into the understanding of how the network underlying early language comprehension develops.

Credit authorship contribution statement

Ting Qi: Conceptualization, Methodology, Formal analysis, Writing – original draft, Writing – review & editing. **Gesa Schaadt:** Conceptualization, Supervision, Writing – review & editing. **Angela D. Friederici:** Conceptualization, Supervision, Project administration, Funding acquisition, Writing – review & editing.

Data and code availability statements

The authors do not have permission to share data according to the ethics agreement. Code is available from the authors upon request.

Acknowledgement

This work was supported by the Max Planck Society (ADF, GS, TQ), the European Research Council (ERC-2010-AdG 20100407, project 269505 NEUROSyntax, awarded to ADF), by the Max Planck Society and the Fraunhofer Society (grant number M.FE.A.NEPF0001). The authors declare to have no conflict of interest. The authors thank Dr. Joshua Grant for proofreading the manuscript.

Supplementary materials

Supplementary material associated with this article can be found in the online version, at doi:10.1016/j.neuroimage.2021.118452.

References

- Amunts, K., Schleicher, A., Ditterich, A., Zilles, K., 2003. Broca's region: cytoarchitectonic asymmetry and developmental changes. *J. Comp. Neurol.* doi:10.1002/cne.10829.
- Behzadi, Y., Restom, K., Liu, J., Liu, T.T., 2007. A component based noise correction method (CompCor) for BOLD and perfusion based fMRI. *Neuroimage* doi:10.1016/j.neuroimage.2007.04.042.
- Brauer, J., Anwender, A., Friederici, A.D., 2011. Neuroanatomical prerequisites for language functions in the maturing brain. *Cereb. Cortex* 21, 459–466. doi:10.1093/cercor/bhq108.
- Brauer, J., Anwender, A., Perani, D., Friederici, A.D., 2013. Dorsal and ventral pathways in language development. *Brain Lang.* 127, 289–295. doi:10.1016/j.bandl.2013.03.001.
- Brauer, J., Friederici, A.D., 2007. Functional Neural Networks of Semantic and Syntactic Processes in the Developing Brain. *J. Cogn. Neurosci.* 19, 1609–1623. doi:10.1162/jocn.2007.19.10.1609.
- Brown, T.T., Jernigan, T.L., 2012. Brain development during the preschool years. *Neuropsychol. Rev.* 22, 313–333. doi:10.1007/s11065-012-9214-1.
- Brown, T.T., Kuperman, J.M., Chung, Y., Erhart, M., McCabe, C., Hagler, D.J., Venkatraman, V.K., Akshoomoff, N., Amaral, D.G., Bloss, C.S., Casey, B.J., Chang, L., Ernst, T.M., Frazier, J.A., Gruen, J.R., Kaufmann, W.E., Kenet, T., Kennedy, D.N., Murray, S.S., Sowell, E.R., Jernigan, T.L., Dale, A.M., 2012. Neuroanatomical assessment of biological maturity. *Curr. Biol.* 22, 1693–1698. doi:10.1016/j.cub.2012.07.002.
- Buckner, R.L., Sepulcre, J., Talukdar, T., Krienen, F.M., Liu, H., Hedden, T., Andrews-Hanna, J.R., Sperling, R.A., Johnson, K.A., 2009. Cortical hubs revealed by intrinsic functional connectivity: mapping, assessment of stability, and relation to Alzheimer's disease. *J. Neurosci.* doi:10.1523/JNEUROSCI.5062-08.2009.
- Cafiero, R., Brauer, J., Anwender, A., Friederici, A.D., 2018. The Concurrence of Cortical Surface Area Expansion and White Matter Myelination in Human Brain Development. *Cereb. Cortex* 29, 827–837. doi:10.1093/cercor/bhy277.
- Catani, M., Jones, D.K., Ffytche, D.H., 2005. Perisylvian language networks of the human brain. *Ann. Neurol.* 57, 8–16. doi:10.1002/ana.20319.
- Dale, A.M., Fischl, B., Sereno, M.I., 1999. Cortical Surface-Based Analysis: I. Segmentation and Surface Reconstruction. *Neuroimage* 9, 179–194. doi:10.1006/nimg.1998.0395.
- Dehaene-Lambertz, G., Hertz-Pannier, L., Dubois, J., Mériaux, S., Roche, A., Sigman, M., Dehaene, S., 2006. Functional organization of perisylvian activation during presentation of sentences in preverbal infants. *Proc. Natl. Acad. Sci. U. S. A.* doi:10.1073/pnas.0606302103.
- Dittmar, M., Abbot-Smith, K., Lieven, E., Tomasello, M., 2008. German children's comprehension of word order and case marking in causative sentences. *Child Dev* doi:10.1111/j.1467-8624.2008.01181.x.
- Enge, A., Friederici, A.D., Skeide, M.A., 2020. A meta-analysis of fMRI studies of language comprehension in children. *Neuroimage* 215, 116858. doi:10.1016/j.neuroimage.2020.116858.
- Fengler, A., Meyer, L., Friederici, A.D., 2016. How the brain attunes to sentence processing: relating behavior, structure, and function. *Neuroimage* doi:10.1016/j.neuroimage.2016.01.012.
- Fengler, A., Meyer, L., Friederici, A.D., 2015. Brain structural correlates of complex sentence comprehension in children. *Dev. Cogn. Neurosci.* 15, 48–57. doi:10.1016/j.dcn.2015.09.004.
- Ferstl, E.C., Neumann, J., Bogler, C., Von Cramon, D.Y., 2008. The extended language network: a meta-analysis of neuroimaging studies on text comprehension. *Hum. Brain Mapp.* doi:10.1002/hbm.20422.
- Fiebach, C.J., Schlesewsky, M., Lohmann, G., Von Cramon, D.Y., Friederici, A.D., 2005. Revisiting the role of Broca's area in sentence processing: syntactic integration versus syntactic working memory. *Hum. Brain Mapp.* doi:10.1002/hbm.20070.
- Fischl, B., Dale, A.M., 2002. Measuring the thickness of the human cerebral cortex from magnetic resonance images. *Proc. Natl. Acad. Sci.* doi:10.1073/pnas.200033797.
- Fischl, B., Sereno, M.I., Dale, A.M., 1999. Cortical surface-based analysis: II: inflation, flattening, and a surface-based coordinate system. *Neuroimage* 9, 195–207. doi:10.1006/nimg.1998.0396.
- Fonov, V., Evans, A.C., Botteron, K., Almli, C.R., McKinstry, R.C., Collins, D.L., 2011. Unbiased average age-appropriate atlases for pediatric studies. *Neuroimage* 54, 313–327. doi:10.1016/j.neuroimage.2010.07.033.
- Friederici, A.D., 2011. The brain basis of language processing: from structure to function. *Physiol. Rev.* doi:10.1152/physrev.00006.2011.
- Friederici, A.D., Brauer, J., Lohmann, G., 2011. Maturation of the language network: from inter- to intrahemispheric connectivities. *PLoS ONE* 6, 1–7. doi:10.1371/journal.pone.0020726.

- Frison, K.J., Williams, S., Howard, R., Frackowiak, R.S.J., Turner, R., 1996. Movement-related effects in fMRI time-series. *Magn. Reson. Med.* doi:10.1002/mrm.1910350312.
- Gabard-Durnam, L.J., O'Muircheartaigh, J., Dirks, N., Dean, D.C., Tottenham, N., Deoni, S., 2018. Human amygdala functional network development: a cross-sectional study from 3 months to 5 years of age. *Dev. Cogn. Neurosci.* doi:10.1016/j.dcn.2018.06.004.
- Galantucci, S., Tartaglia, M.C., Wilson, S.M., Henry, M.L., Filippi, M., Agosta, F., Dronkers, N.F., Henry, R.G., Ogar, J.M., Miller, B.L., Gorno-Tempini, M.L., 2011. White matter damage in primary progressive aphasia: a diffusion tensor tractography study. *Brain* 134, 3011–3029. doi:10.1093/brain/awr099.
- Ghosh, S.S., Kakunoori, S., Augustinack, J., Nieto-Castanon, A., Kovelman, I., Gaab, N., Christodoulou, J.A., Triantafyllou, C., Gabrieli, J.D.E., Fischl, B., 2010. Evaluating the validity of volume-based and surface-based brain image registration for developmental cognitive neuroscience studies in children 4 to 11 years of age. *Neuroimage* doi:10.1016/j.neuroimage.2010.05.075.
- Gilmore, J.H., Knickmeyer, R.C., Gao, W., 2018. Imaging structural and functional brain development in early childhood. *Nat. Rev. Neurosci.* doi:10.1038/nrn.2018.1.
- Glasser, M.F., Coalson, T.S., Robinson, E.C., Hacker, C.D., Harwell, J., Yacoub, E., Ugurbil, K., Andersson, J., Beckmann, C.F., Jenkinson, M., Smith, S.M., Van Essen, D.C., 2016. A multi-modal parcellation of human cerebral cortex. *Nature* doi:10.1038/nature18933.
- Gogtay, N., Giedd, J.N., Lusk, L., Hayashi, K.M., Greenstein, D., Vaituzis, A.C., Nugent, T.F., Herman, D.H., Clasen, L.S., Toga, A.W., Rapoport, J.L., Thompson, P.M., 2004. Dynamic mapping of human cortical development during childhood through early adulthood. *Proc. Natl. Acad. Sci. U. S. A.* doi:10.1073/pnas.0402680101.
- Grady, C.L., Rieck, J.R., Nichol, D., Rodrigue, K.M., Kennedy, K.M., 2021. Influence of sample size and analytic approach on stability and interpretation of brain-behavior correlations in task-related fMRI data. *Hum. Brain Mapp.* doi:10.1002/hbm.25217.
- Han, X., Jovicich, J., Salat, D., van der Kouwe, A., Quinn, B., Czanner, S., Busa, E., Pacheco, J., Albert, M., Killiany, R., Maguire, P., Rosas, D., Makris, N., Dale, A., Dickerson, B., Fischl, B., 2006. Reliability of MRI-derived measurements of human cerebral cortical thickness: the effects of field strength, scanner upgrade and manufacturer. *Neuroimage* 32, 180–194. doi:10.1016/j.neuroimage.2006.02.051.
- Harms, M.P., Somerville, L.H., Ances, B.M., Andersson, J., Barch, D.M., Bastiani, M., Bookheimer, S.Y., Brown, T.B., Buckner, R.L., Burgess, G.C., Coalson, T.S., Chappell, M.A., Dapretto, M., Douaud, G., Fischl, B., Glasser, M.F., Greve, D.N., Hodge, C., Jamison, K.W., Jbabdi, S., Kandal, S., Li, X., Mair, R.W., Mangia, S., Marcus, D., Mascali, D., Moeller, S., Nichols, T.E., Robinson, E.C., Salat, D.H., Smith, S.M., Sotiropoulos, S.N., Terpe, M., Thomas, K.M., Tisdall, M.D., Ugurbil, K., van der Kouwe, A., Woods, R.P., Zöllei, L., Van Essen, D.C., Yacoub, E., 2018. Extending the human connectome project across ages: imaging protocols for the lifespan development and aging projects. *Neuroimage* 183, 972–984. doi:10.1016/j.neuroimage.2018.09.060.
- Hill, J., Inder, T., Neil, J., Dierker, D., Harwell, J., Van Essen, D., 2010. Similar patterns of cortical expansion during human development and evolution. *Proc. Natl. Acad. Sci. U. S. A.* doi:10.1073/pnas.1001229107.
- Holland, S.K., Vannest, J., Mecoli, M., Jacola, L.M., Tillema, J.M., Karunanayaka, P.R., Schmithorst, V.J., Yuan, W., Plante, E., Byars, A.W., 2007. Functional MRI of language lateralization during development in children. *Int. J. Audiol.* doi:10.1080/14992020701448994.
- Jenkinson, M., Bannister, P., Brady, M., Smith, S., 2002. Improved optimization for the robust and accurate linear registration and motion correction of brain images. *Neuroimage* doi:10.1016/S1053-8119(02)91132-8.
- Karunanayaka, P.R., Holland, S.K., Schmithorst, V.J., Solodkin, A., Chen, E.E., Szafarski, J.P., Plante, E., 2007. Age-related connectivity changes in fMRI data from children listening to stories. *Neuroimage* doi:10.1016/j.neuroimage.2006.08.028.
- Kaufman, A.S., 2004. *Manual For the Kaufman Assessment Battery for Children (K-ABC-II)*. Circ. Pines, MN AGS.
- Kaufman, A.S., Kaufman, N.L., 1983. *Kaufman Assessment Battery For Children*. Wiley Online Library.
- Kebets, V., Holmes, A.J., Orban, C., Tang, S., Li, J., Sun, N., Kong, R., Poldrack, R.A., Yeo, B.T.T., 2019. Somatosensory-motor dysconnectivity spans multiple transdiagnostic dimensions of psychopathology. *Biol. Psychiatry* 86, 779–791. doi:10.1016/j.biopsych.2019.06.013.
- Knoll, L.J., Obleser, J., Schipke, C.S., Friederici, A.D., Brauer, J., 2012. Left prefrontal cortex activation during sentence comprehension covaries with grammatical knowledge in children. *Neuroimage* doi:10.1016/j.neuroimage.2012.05.014.
- Krishnan, A., Williams, L.J., McIntosh, A.R., Abdi, H., 2011. Partial Least Squares (PLS) methods for neuroimaging: a tutorial and review. *Neuroimage* doi:10.1016/j.neuroimage.2010.07.034.
- Kuhl, U., Neef, N.E., Kraft, I., Schaadt, G., Dörr, L., Brauer, J., Czepezauer, I., Müller, B., Wilcke, A., Kirsten, H., Emmrich, F., Boltze, J., Friederici, A.D., Skeide, M.A., 2020. The emergence of dyslexia in the developing brain. *Neuroimage* 211. doi:10.1016/j.neuroimage.2020.116633.
- Leff, A.P., Schofield, T.M., Crinion, J.T., Seghier, M.L., Grogan, A., Green, D.W., Price, C.J., 2009. The left superior temporal gyrus is a shared substrate for auditory short-term memory and speech comprehension: evidence from 210 patients with stroke. *Brain* doi:10.1093/brain/awp273.
- Lays, C., Ley, C., Klein, O., Bernard, P., Licata, L., 2013. Detecting outliers: do not use standard deviation around the mean, use absolute deviation around the median. *J. Exp. Soc. Psychol.* 49, 764–766. doi:10.1016/j.jesp.2013.03.013.
- Lindner, K., 2003. The development of sentence-interpretation strategies in monolingual German-learning children with and without specific language impairment. *Linguistics* doi:10.1515/ling.2003.008.
- Long, X., Benischek, A., Dewey, D., Lebel, C., 2017. Age-related functional brain changes in young children. *Neuroimage* doi:10.1016/j.neuroimage.2017.04.059.
- Lu, L.H., Leonard, C.M., Thompson, P.M., Kan, E., Jolley, J., Welcome, S.E., Toga, A.W., Sowell, E.R., 2007. Normal developmental changes in inferior frontal gray matter are associated with improvement in phonological processing: a longitudinal MRI analysis. *Cereb. Cortex* doi:10.1093/cercor/bhl019.
- Lukic, A.S., Wernick, M.N., Strother, S.C., 2002. An evaluation of methods for detecting brain activations from functional neuroimages. *Artif. Intell. Med.* 25, 69–88. doi:10.1016/S0933-3657(02)00009-X.
- Määttä, S., Laakso, M.L., Tolvanen, A., Ahonen, T., Aro, T., 2014. Children with differing developmental trajectories of prelinguistic communication skills: language and working memory at age 5. *J. Speech, Lang. Hear. Res.* doi:10.1044/2014_JSLHR-L1-13-0012.
- Makuuchi, M., Friederici, A.D., 2013. Hierarchical functional connectivity between the core language system and the working memory system. *Cortex* doi:10.1016/j.cortex.2013.01.007.
- Marek, S., Tervo-Clemmens, B., Nielsen, A.N., Wheelock, M.D., Miller, R.L., Laumann, T.O., Earl, E., Foran, W.W., Cordova, M., Doyle, O., Perrone, A., Miranda-Dominguez, O., Fezko, E., Sturgeon, D., Graham, A., Hermsillo, R., Snider, K., Galassi, A., Nagel, B.J., Ewing, S.W.F., Eggebrecht, A.T., Garavan, H., Dale, A.M., Greene, D.J., Barch, D.M., Fair, D.A., Luna, B., Dosenbach, N.U.F., 2019. Identifying reproducible individual differences in childhood functional brain networks: an ABCD study. *Dev. Cogn. Neurosci.* 40, 100706. doi:10.1016/j.dcn.2019.100706.
- McIntosh, A.R., Bookstein, F.L., Haxby, J.V., Grady, C.L., 1996. Spatial pattern analysis of functional brain images using partial least squares. *Neuroimage* doi:10.1006/nimg.1996.0016.
- McIntosh, A.R., Lobaugh, N.J., 2004. Partial least squares analysis of neuroimaging data: applications and advances. *Neuroimage* doi:10.1016/j.neuroimage.2004.07.020.
- McIntosh, A.R., Mišić, B., 2013. Multivariate statistical analyses for neuroimaging data. *Annu. Rev. Psychol.* doi:10.1146/annurev-psych-113011-143804.
- Meyer, L., Obleser, J., Anwender, A., Friederici, A.D., 2012. Linking ordering in Broca's area to storage in left temporo-parietal regions: the case of sentence processing. *Neuroimage* doi:10.1016/j.neuroimage.2012.05.052.
- Montgomery, J.W., Magimairaj, B.M., O'Malley, M.H., 2008. Role of working memory in typically developing children's complex sentence comprehension. *J. Psycholinguist. Res.* doi:10.1007/s10936-008-9077-z.
- Natu, V.S., Gomez, J., Barnett, M., Jeska, B., Kirilina, E., Jaeger, C., Zhen, Z., Cox, S., Weiner, K.S., Weiskopf, N., Grill-Spector, K., 2019. Apparent thinning of human visual cortex during childhood is associated with myelination. *Proc. Natl. Acad. Sci. U. S. A.* doi:10.1073/pnas.1904931116.
- Newman, S.D., Just, M.A., Keller, T.A., Roth, J., Carpenter, P.A., 2003. Differential effects of syntactic and semantic processing on the subregions of Broca's area. *Cogn. Brain Res.* doi:10.1016/S0926-6410(02)00285-9.
- Nichols, T., Hayasaka, S., 2003. Controlling the familywise error rate in functional neuroimaging: a comparative review. *Stat. Methods Med. Res.* doi:10.1191/0962280203sm341ra.
- Nimon, K., Lewis, M., Kane, R., Haynes, R.M., 2008. An R package to compute commonality coefficients in the multiple regression case: an introduction to the package and a practical example. *Behav. Res. Methods* doi:10.3758/BRM.40.2.457.
- Novais-Santos, S., Gee, J., Shah, M., Troiani, V., Work, M., Grossman, M., 2007. Resolving sentence ambiguity with planning and working memory resources: evidence from fMRI. *Neuroimage* doi:10.1016/j.neuroimage.2007.03.077.
- Nuñez, S.C., Dapretto, M., Katzir, T., Starr, A., Bramer, J., Kan, E., Bookheimer, S., Sowell, E.R., 2011. fMRI of syntactic processing in typically developing children: structural correlates in the inferior frontal gyrus. *Dev. Cogn. Neurosci.* 1, 313–323. doi:10.1016/j.dcn.2011.02.004.
- Obleser, J., Wise, R.J.S., Dresner, M.A., Scott, S.K., 2007. Functional integration across brain regions improves speech perception under adverse listening conditions. *J. Neurosci.* doi:10.1523/JNEUROSCI.4663-06.2007.
- Oldfield, R.C., 1971. The assessment and analysis of handedness: the Edinburgh inventory. *Neuropsychologia* 9, 97–113. doi:10.1016/0028-3932(71)90067-4.
- Owen, A.M., McMillan, K.M., Laird, A.R., Bullmore, E., 2005. N-back working memory paradigm: a meta-analysis of normative functional neuroimaging studies. In: *Human Brain Mapping*. Hum Brain Mapp, pp. 46–59. doi:10.1002/hbm.20131.
- Perani, D., Sacchunan, M.C., Scifo, P., Anwender, A., Spada, D., Baldoli, C., Poloniato, A., Lohmann, G., Friederici, A.D., 2011. Neural language networks at birth. *Proc. Natl. Acad. Sci.* 108, 16056–16061. doi:10.1073/pnas.1102991108.
- Petanjek, Z., Judaš, M., Šimić, G., Rašin, M.R., Uylings, H.B.M., Rakic, P., Kostović, I., 2011. Extraordinary neoteny of synaptic spines in the human prefrontal cortex. *Proc. Natl. Acad. Sci. U. S. A.* doi:10.1073/pnas.1105108108.
- Petermann, F., Petermann, U., 2011. *Wechsler Intelligence Scale For Children (WISC-IV)*. Power, J.D., Barnes, K.A., Snyder, A.Z., Schlaggar, B.L., Petersen, S.E., 2012. Spurious but systematic correlations in functional connectivity MRI networks arise from subject motion. *Neuroimage* doi:10.1016/j.neuroimage.2011.10.018.
- Prunier, J.G., Colyn, M., Legendre, X., Nimon, K.F., Flamand, M.C., 2015. Multicollinearity in spatial genetics: separating the wheat from the chaff using commonality analyses. *Mol. Ecol.* doi:10.1111/mec.13029.
- Qi, T., Schaadt, G., Cafero, R., Brauer, J., Skeide, M.A., Friederici, A.D., 2019a. The emergence of long-range language network structural covariance and language abilities. *Neuroimage* 191, 36–48. doi:10.1016/j.neuroimage.2019.02.014.
- Qi, T., Schaadt, G., Friederici, A.D., 2019b. Cortical thickness lateralization and its relation to language abilities in children. *Dev. Cogn. Neurosci.* 39, 100704. doi:10.1016/j.dcn.2019.100704.
- Ray-Mukherjee, J., Nimon, K., Mukherjee, S., Morris, D.W., Slotow, R., Hamer, M., 2014. Using commonality analysis in multiple regressions: a tool to decompose regression effects in the face of multicollinearity. *Methods Ecol. Evol.* doi:10.1111/2041-210X.12166.

- Raznahan, A., Lerch, J.P., Lee, N., Greenstein, D., Wallace, G.L., Stockman, M., Clasen, L., Shaw, P.W., Giedd, J.N., 2011. Patterns of coordinated anatomical change in human cortical development: a longitudinal neuroimaging study of maturational coupling. *Neuron* 72, 873–884. doi:10.1016/j.neuron.2011.09.028.
- Redcay, E., Haist, F., Courchesne, E., 2008. Paper: functional neuroimaging of speech perception during a pivotal period in language acquisition. *Dev. Sci.* doi:10.1111/j.1467-7687.2008.00674.x.
- Reynolds, J.E., Long, X., Grohs, M.N., Dewey, D., Lebel, C., 2019. Structural and functional asymmetry of the language network emerge in early childhood. *Dev. Cogn. Neurosci.* 39, 100682. doi:10.1016/j.dcn.2019.100682.
- Richardson, F.M., Thomas, M.S.C., Filippi, R., Harth, H., Price, C.J., 2010. Contrasting effects of vocabulary knowledge on temporal and parietal brain structure across lifespan. *J. Cogn. Neurosci.* 22, 943–954. doi:10.1162/jocn.2009.21238.
- Roehrich-Gascon, D., Small, S.L., Tremblay, P., 2015. Structural correlates of spoken language abilities: a surface-based region-of interest morphometry study. *Brain Lang* doi:10.1016/j.bandl.2015.06.004.
- Schmithorst, V.J., Holland, S.K., Plante, E., 2006. Cognitive modules utilized for narrative comprehension in children: a functional magnetic resonance imaging study. *Neuroimage* doi:10.1016/j.neuroimage.2005.07.020.
- Siegmüller, J., Kauschke, C., von Minnen, S., Bittner, D., 2011. TSVK Test Zum Satzverstehen von Kindern.
- Skeide, M.A., Brauer, J., Friederici, A.D., 2016. Brain Functional and Structural Predictors of Language Performance. *Cereb. Cortex*. doi:10.1093/cercor/bhv042.
- Skeide, M.A., Brauer, J., Friederici, A.D., 2014. Syntax gradually segregates from semantics in the developing brain. *Neuroimage* 100, 106–111. doi:10.1016/j.neuroimage.2014.05.080.
- Skeide, M.A., Friederici, A.D., 2016. The ontogeny of the cortical language network. *Nat. Rev. Neurosci.* doi:10.1038/nrn.2016.23.
- Sowell, E.R., Thompson, P.M., Leonard, C.M., Welcome, S.E., Kan, E., Toga, A.W., 2004. Longitudinal mapping of cortical thickness and brain growth in normal children. *J. Neurosci.* 24, 8223–8231. doi:10.1523/JNEUROSCI.1798-04.2004.
- Szaflarski, J.P., Altaye, M., Rajagopal, A., Eaton, K., Meng, X.X., Plante, E., Holland, S.K., 2012. A 10-year longitudinal fMRI study of narrative comprehension in children and adolescents. *Neuroimage* 63, 1188–1195. doi:10.1016/j.neuroimage.2012.08.049.
- Tamnes, C.K., Herting, M.M., Goddings, A.L., Meuwese, R., Blakemore, S.J., Dahl, R.E., Güroğlu, B., Raznahan, A., Sowell, E.R., Crone, E.A., Mills, K.L., 2017. Development of the cerebral cortex across adolescence: a multisample study of inter-related longitudinal changes in cortical volume, surface area, and thickness. *J. Neurosci.* doi:10.1523/JNEUROSCI.3302-16.2017.
- Thompson-schill, S.L., Ramscar, M., Chrysikou, E.G., 2009. When a little frontal lobe goes a long way. *Psychol. Sci.* 18, 259–263. doi:10.1111/j.1467-8721.2009.01648.x.
- Van Dijk, K.R.A., Hedden, T., Venkataraman, A., Evans, K.C., Lazar, S.W., Buckner, R.L., 2010. Intrinsic functional connectivity as a tool for human connectomics: theory, properties, and optimization. *J. Neurophysiol.* 103, 297–321. doi:10.1152/jn.00783.2009.
- Vigneau, M., Beaucousin, V., Hervé, P.Y., Duffau, H., Crivello, F., Houdé, O., Mazoyer, B., Tzourio-Mazoyer, N., 2006. Meta-analyzing left hemisphere language areas: phonology, semantics, and sentence processing. *Neuroimage* doi:10.1016/j.neuroimage.2005.11.002.
- Vissienon, K., Friederici, A.D., Brauer, J., Wu, C.-Y., 2017. Functional organization of the language network in three- and six-year-old children. *Neuropsychologia* 98, 24–33.
- Wang, J., Rice, M.L., Booth, J.R., 2019. Syntactic and semantic specialization and integration in 5-to 6-year-old children during auditory sentence processing. *J. Cogn. Neurosci.* doi:10.1162/jocn_a_01477.
- Weighall, A.R., Altmann, G.T.M., 2011. The role of working memory and contextual constraints in children's processing of relative clauses. *J. Child Lang.* doi:10.1017/S0305000910000267.
- Weiss-Croft, L.J., Baldeweg, T., 2015. Maturation of language networks in children: a systematic review of 22years of functional MRI. *Neuroimage* doi:10.1016/j.neuroimage.2015.07.046.
- Wilson, S.M., Galantucci, S., Tartaglia, M.C., Rising, K., Patterson, D.K., Henry, M.L., Ogar, J.M., DeLeon, J., Miller, B.L., Gorno-Tempini, M.L., 2011. Syntactic processing depends on dorsal language tracts. *Neuron* 72, 397–403. doi:10.1016/j.neuron.2011.09.014.
- Worsley, K.J., Andermann, M., Koulis, T., MacDonald, D., Evans, A.C., 1999. Detecting changes in nonisotropic images. *Hum. Brain Mapp.* https://doi.org/10.1002/(SICI)1097-0193(1999)8:2/3<98::AID-HBM5>3.0.CO;2-F.
- Wu, C.Y., Vissienon, K., Friederici, A.D., Brauer, J., 2016. Preschoolers' brains rely on semantic cues prior to the mastery of syntax during sentence comprehension. *Neuroimage* 126, 256–266. doi:10.1016/j.neuroimage.2015.10.036.
- Xiang, H.D., Fontijn, H.M., Norris, D.G., Hagoort, P., 2010. Topographical functional connectivity pattern in the perisylvian language networks. *Cereb. Cortex*. doi:10.1093/cercor/bhp119.
- Xiao, Y., Friederici, A.D., Margulies, D.S., Brauer, J., 2016a. Development of a selective left-hemispheric fronto-temporal network for processing syntactic complexity in language comprehension. *Neuropsychologia* doi:10.1016/j.neuropsychologia.2015.09.003.
- Xiao, Y., Friederici, A.D., Margulies, D.S., Brauer, J., 2016b. Longitudinal changes in resting-state fMRI from age 5 to age 6years covary with language development. *Neuroimage* doi:10.1016/j.neuroimage.2015.12.008.
- Xu, J., Kemeny, S., Park, G., Fratalli, C., Braun, A., 2005. Language in context: emergent features of word, sentence, and narrative comprehension. *Neuroimage* doi:10.1016/j.neuroimage.2004.12.013.
- Yan, C.-G., Cheung, B., Kelly, C., Colcombe, S., Craddock, R.C., Di Martino, A., Li, Q., Zuo, X.-N., Castellanos, F.X., Milham, M.P., 2013. A comprehensive assessment of regional variation in the impact of head micromovements on functional connectomics. *Neuroimage* 76, 183–201. doi:10.1016/j.neuroimage.2013.03.004.
- Yarkoni, T., Poldrack, R.A., Nichols, T.E., Essen, D.C.Van, Wager, T.D., 2011. NeuroSynth: a new platform for large-scale automated synthesis of human functional neuroimaging data. *Front. Neuroinform.* 5. doi:10.3389/conf.fninf.2011.08.00058.
- Yeatman, J.D., Ben-Shachar, M., Glover, G.H., Feldman, H.M., 2010. Individual differences in auditory sentence comprehension in children: an exploratory event-related functional magnetic resonance imaging investigation. *Brain Lang.* doi:10.1016/j.bandl.2009.11.006.
- Zöllner, D., Sandini, C., Karahanoglu, F.I., Padula, M.C., Schaefer, M., Eliez, S., Van De Ville, D., 2019. Large-scale brain network dynamics provide a measure of psychosis and anxiety in 22q11.2 deletion syndrome. *Biol. Psychiatry Cogn. Neurosci. Neuroimaging* 4, 881–892. doi:10.1016/j.bpsc.2019.04.004.
- Zöllner, D., Schaefer, M., Scariati, E., Padula, M.C., Eliez, S., Van De Ville, D., 2017. Disentangling resting-state BOLD variability and PCC functional connectivity in 22q11.2 deletion syndrome. *Neuroimage* doi:10.1016/j.neuroimage.2017.01.064.
- Zuo, X.N., Kelly, C., Adelstein, J.S., Klein, D.F., Castellanos, F.X., Milham, M.P., 2010. Reliable intrinsic connectivity networks: test-retest evaluation using ICA and dual regression approach. *Neuroimage* doi:10.1016/j.neuroimage.2009.10.080.
- Zuo, X.N., Xu, T., Jiang, L., Yang, Z., Cao, X.Y., He, Y., Zang, Y.F., Castellanos, F.X., Milham, M.P., 2013. Toward reliable characterization of functional homogeneity in the human brain: preprocessing, scan duration, imaging resolution and computational space. *Neuroimage* doi:10.1016/j.neuroimage.2012.10.017.